ELSEVIER

Journal of Organometallic Chemistry 557 (1998) 3–12

Journal of Organometallic Chemistry

Half-sandwich complexes of niobium and tantalum bearing *o*-xylylene, anthracene, or cyclooctatetraene: crystal structures of $(\eta^5\text{-}C_5Me_5)Nb\{o\text{-}(CH_2)_2C_6H_4\}Cl_2$, $(\eta^5\text{-}C_5Me_5)Ta(\eta^4\text{-anthracene})(CH_2Ph)_2$, and $(\eta^5\text{-}C_5Me_5)Nb(\eta^4\text{-butadiene})(\eta^3\text{-cyclooctatetraene})$

Kazushi Mashima [a,*], Yuushou Nakayama [b], Michitaka Kaidzu [b], Naoko Ikushima [b], Akira Nakamura [b]

[a] *Department of Chemistry, Graduate School of Engineering Science, Osaka University, Toyonaka, Osaka, 560, Japan*
[b] *Department of Macromolecular Science, Graduate School of Science, Osaka University, Toyonaka, Osaka, 560, Japan*

Received 17 June 1997; received in revised form 25 August 1997

Abstract

Half-sandwich complexes of niobium and tantalum having an extended conjugated 1,3-diene ligand such as *o*-xylylene, anthracene, and cyclooctatetraene have been synthesized and characterized. The molecular structures of $Cp^*Nb\{o\text{-}(CH_2)_2C_6H_4\}Cl_2$ (**1**) ($Cp^* = \eta^5$-pentamethylcyclopentadienyl), $Cp^*Ta(\eta^4\text{-}C_{14}H_{10})(CH_2Ph)_2$ (**14**), and $Cp^*Nb(\eta^4\text{-}C_4H_6)(\eta^3\text{-}C_8H_8)$ (**16**) were determined by X-ray crystallographic studies. Complexes **1** and **14** adopted a four-legged piano stool geometry and their *o*-xylylene and anthracene ligands coordinated to the metal center in the η^4-coordination mode. X-ray analysis together with their NMR spectral data revealed that the *o*-xylylene complex **1** has a large contribution of the $2\sigma-1\pi$ canonical form, but otherwise the anthracene complexes have an increased contribution of $2\pi-\eta^4$-diene canonical form compared with the butadiene complexes. Thus, the electronic structures of η^4-*o*-xylylene and η^4-anthracene ligands are deviated from that of η^4-butadiene into the opposite direction. The ^{1}H NMR singlet signal of the cyclooctatetraene ligand in **16** indicated the presence of the dynamic fluxionality in solution, while it coordinated to the metal in η^3-fashion in the crystal. © 1998 Elsevier Science S.A. All rights reserved.

Keywords: Tantalum; Niobium; *o*-xylylene; Anthracene; Cyclooctatetraene; Crystal structure

1. Introduction

Conjugated dienes have been used among the most useful and attractive ligands in organometallic chemistry [1–6]. We and colleagues have been interested in chemistry of conjugated 1,3-diene complexes of early transition metals, e.g. Cp_2M(diene) (M = Ti, Zr, Hf; Cp = cyclopentadienyl derivatives) [7,8], CpM(diene)X (M = Ti, Zr, Hf; X = Cl, Br, I, alkyl) [7,9,10], $CpM(diene)_2$ (M = Nb, Ta) [11–13], and $CpM(diene)X_2$ (M = Nb, Ta; X = Cl, alkyl, aryl, etc.) [11,13], in which the diene ligands are best described as having both contributions of neutral $2\pi-\eta^4$-diene and formally dianionic $2\sigma-1\pi$ canonical forms. Our recent interest in diene complexes of group 5 metals stems from their unique catalytic ability similar to group 4 metallocene complexes for the polymerization of ethylene and norbornene [14–20]. Thus, it would be our target to investigate the electronic and steric effects of the diene ligands on these Group 5 transition metals. In this connection, we chose *o*-xylylene (*o*-quinodimethane), anthracene, and cyclooctatetraene as alternative η^4-1,3-diene ligands having the extended pπ-conjugation

---

[*] Corresponding author. Tel.: +81 6 8506247; fax: +81 6 8506296; e-mail: mashima@chem.es.osaka-u.ac.jp

PII S0022-328X(97)00730-4

Table 1
A comparison of bonding features indicated by NMR and X-ray studies

Complex	n (sp^n hybridization)[a]		θ (°)[b]	Δd (Å)[c]	Δl (Å)[d]	ref.
	$C_{1,4}$	$C_{2,3}$				
$Cp^*Nb(xylylene)Cl_2$ (**1**)	2.45	—	101.9	−0.312	0.041	this work
$\{C_5H_4(SiMe_3)\}_2Nb(xylylene)$ (**6**)	—	—	136	−0.79	0.095	[28]
$Cp_2M(xylylene)$ (M = Ti, Zr, Hf, Nb)						[26,28]
M = Ti (**7**)	—	—	139	−0.71	0.081	
M = Zr (**8**)	—	—	127	−0.56	0.053	
M = Hf (**9**)	—	—	127	−0.63	0.09	
$Cp^*Ti(xylylene)Cl$ (**10**)	2.51	—	—	—	—	[49]
$\{Cp^*Ti(xylylene)\}_2(\mu\text{-xylylene})$ (**11**)						[27]
Terminal	2.60	—	109.5	−0.35	0.045	
Bridging	3.09	—	—	—	0.055	
$W(xylylene)_3$ (**6**)	—	—	—	−0.275	0.04	[29]
$Cp^*Ta(anthracene)Cl_2$ (**12**)	2.33	1.95	—	—	—	this work
$Cp^*Ta(anthracene)(CH_2Ph)_2$ (**14**)	—	—	85.9	−0.041	0.083	this work
$Cp^*Ta(C_4H_6)Cl_2$ (**13**)	2.35	2.04				[13]
$CpTa(C_4H_6)Cl_2$ (**21**)	2.47	2.04	94.9	−0.160	0.081	[13]
$Cp^*Ta(C_4H_6)(CH_2Ph)_2$ (**15**)	2.38	2.05	93.3	−0.127	0.050	[15]
$Cp^*Nb(C_4H_6)(cot)$ (**16**)	2.41	2.14	101.9	−0.120	0.037	this work
$Cp^*(C_4H_6)\overline{Nb[CH_2CH(C_5H_8)C}H]$ (**3**)	2.44	2.15	92.6	−0.12	−0.005	[14]
$CpNb(C_4H_6)(\eta^2\text{-MeC}\equiv\text{CPh})(PMe_3)$ (**5**)	2.35	2.16	84.0	0.049	0.024	[22]
CpNb(2,3-dimethylbutadiene)$_2$ (**4**)						[11]
Supine	2.49	—	101.1	−0.23	0.073	
Prone	2.38	—	98.7	−0.14	0.019	

[a] Estimated by using Newton's empirical law [21] from the $^1J_{CH}$ coupling constant.
[b] θ denotes the dihedral angle between M–C(1)–C(4) and C(1)–C(2)–C(3)–C(4) planes.
[c] $\Delta d = [d(M-C(1)) + d(M-C(4))]/2 - [d(M-C(2)) + d(M-C(3))]/2$.
[d] $\Delta l = [d(C(1)-C(2)) + d(C(3)-C(4))]/2 - d(C(2)-C(3))$.

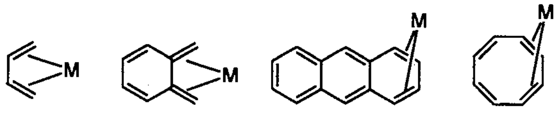

Scheme 1.

(Scheme 1). Herein we report the syntheses and characterization of half-sandwich complexes of niobium and tantalum bearing a conjugated-diene ligand such as *o*-xylylene, anthracene, and cyclooctatetraene.

2. Results and discussion

2.1. Preparation and characterization of a niobium *o*-xylylene complex, $Cp^*Nb\{o\text{-}(CH_2)_2C_6H_4\}Cl_2$ (*1*)

Reaction of Cp^*NbCl_4 ($Cp^* = \eta^5$-pentamethylcyclopentadienyl) with $o\text{-}C_6H_4(CH_2MgCl)_2$ gave an *o*-xylylene complex of niobium, $Cp^*Nb\{o\text{-}(CH_2)_2C_6H_4\}Cl_2$ (**1**), in 16% yield as green crystals (Eq. (1)); its constitution was supported by elemental analysis as well as by NMR spectroscopy. The α-protons of the *o*-xylylene ligand in the ^1H NMR spectrum of **1** were observed as an AB-type quartet at δ 0.75 and 1.95; a resonance of α-carbons appeared at δ 71.3 with a $^1J_{CH}$ coupling constant of 147 Hz. Thus the extent of sp^n hybridization of the α-carbon of the *o*-xylylene ligand in **1** was estimated by using Newton's empirical law [21] to be $n = 2.45$, showing relatively higher p-character compared to those of the butadiene ligand in the typical niobium monokis(butadiene) complexes reported so far (see Table 1) [14,22]. In the reaction course, the corresponding bis(xylylene) complex such as $Cp^*Nb\{o\text{-}(CH_2)_2C_6H_4\}_2$ was not detected at all; being in contrast to a general trend that preparation of monokis(diene)complexes [11] was often accompanied by the formation of small amounts of the corresponding bis(diene)complexes.

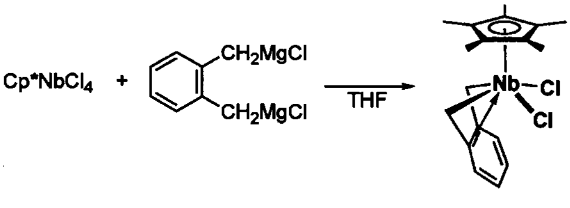

(1)

1

The molecular structure of **1** determined by X-ray crystallography is shown in Fig. 1. The selected bond

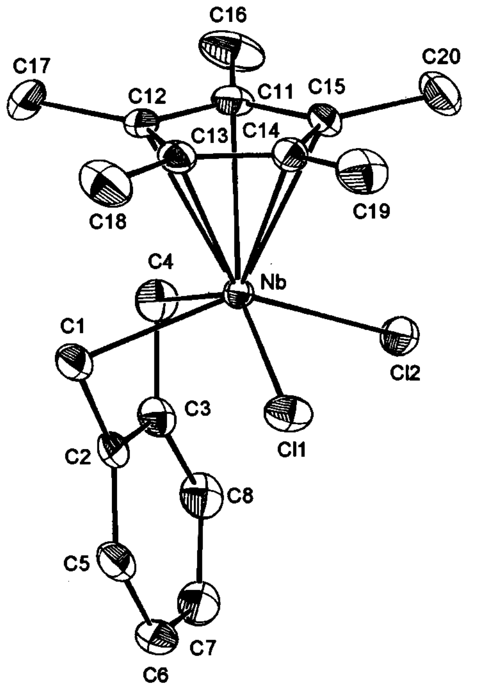

Fig. 1. ORTEP drawing of $Cp^*Nb\{o\text{-}(CH_2)_2C_6H_4\}Cl_2$ (**1**) with the numbering scheme.

distances and angles are listed in Table 2. The *o*-xylylene ligand has been reported to coordinate to the transition metal in a variety of fashions as shown in Scheme 2 [23,24]. Metallocene-type complexes of Ti, Zr, Hf and Nb have been reported to have a metallacyclopentene structure (type A in Scheme 2) [25,26], while a half-metallocene of titanium adopted an η^4-*o*-xylylene type B in Scheme 2 [27]. Complex **1** also has the type B structure and adopts a four legged piano stool geometry comprised of a capping Cp* ligand together with two carbon atoms of the *o*-xylylene ligand and two chlorine atoms as four legs. The Nb–C(1) (2.240(5) Å) and Nb–C(4) (2.236(5) Å) distances of **1** are slightly shorter than those of the butadiene ligands in $Cp^*(\eta^4\text{-}C_4H_6)\overline{Nb[CH_2CH(C_5H_8)CH]}$ (**2**) (2.26(1) and 2.28(1) Å) [14], $CpNb(\eta^4\text{-}C_4H_6)(MeC{\equiv}CPh)(PMe_3)$ (**3**) (2.406(1) and 2.391(1) Å) [22] and $CpNb(\eta^4\text{-}2,3\text{-dimethylbutadiene})_2$ (**4**) (*supine*, 2.286(8) Å; *prone* 2.324(8) Å) [11], and also shorter than that found for an *o*-xylylene complex of niobocene, $\{C_5H_4(SiMe_3)\}_2Nb(xylylene)$ (**5**) (av. 2.286 Å) [28]. The Nb–C(2) (2.544(4) Å) and Nb–C(3) (2.556(4) Å) distances of **1** are significantly longer than those of the butadiene ligands in **2** (2.40(1) and 2.38(1) Å), **3** (2.354(1) and 2.345(1) Å) and **4** (*supine*, 2.519(7) Å; *prone* 2.467(7) Å), but far shorter than that of **5** (av. 3.079 Å) in which there are no bonding interaction between the niobium atom and the C_β carbons, C(2) and C(3). The C(1)–C(2) (1.457(7) Å), C(2)–C(3) (1.415(6) Å), and C(3)–C(4) (1.455(7) Å) bond distances show long-short-long bond alternation, though the difference is smaller than that in the butadiene complexes. The long-short-long-short-long bond alternation within aromatic ring system, i.e. C(2)–C(5) (1.412(7) Å), C(5)–C(6) (1.368(7) Å), C(6)–C(7) (1.396(8) Å), C(7)–C(8) (1.358(8) Å) and C(8)–C(3) (1.407(7) Å), indicates the electron localization in the aromatic moiety of the xylylene ligand; similar bond alternation has been observed in $W(xylylene)_3$ (**6**) [29]. The large dihedral angle (101.87°) between Nb–C(1)–C(4) and C(1)–C(2)–C(3)–C(4) planes (θ), of **1** is larger by ca. 10° than that of typical niobium mono(butadiene) complexes [14,22]. This large fold angle is

Table 2
Selected bond distances (Å) and angles (°) of **1**

Bond distances (Å)			
Nb–Cl(1)	2.409(1)	Nb–Cl(2)	2.419(1)
Nb–C(1)	2.240(5)	Nb–C(2)	2.544(4)
Nb–C(3)	2.556(4)	Nb–C(4)	2.236(5)
Nb–C(11)	2.434(4)	Nb–C(12)	2.445(5)
Nb–C(13)	2.421(4)	Nb–C(14)	2.416(4)
Nb–C(15)	2.420(4)	C(1)–C(2)	1.457(7)
C(2)–C(3)	1.415(6)	C(3)–C(4)	1.455(7)
C(2)–C(5)	1.412(7)	C(5)–C(6)	1.368(7)
C(6)–C(7)	1.396(8)	C(7)–C(8)	1.358(8)
C(3)–C(8)	1.407(7)		
Bond angles (°)			
Cl(1)–Nb–Cl(2)	92.58(5)	Cl(1)–Nb–C(1)	83.8(2)
Cl(1)–Nb–C(4)	138.9(2)	Cl(2)–Nb–C(1)	137.9(1)
Cl(2)–Nb–C(4)	84.2(2)	C(1)–Nb–C(4)	72.2(2)
Nb–C(1)–C(2)	84.1(3)	Nb–C(4)–C(3)	84.9(3)
C(1)–C(2)–C(3)	115.4(5)	C(2)–C(3)–C(4)	114.2(5)
Fold angles of the best planes (°)			
$\theta(1)^a$	101.87	$\theta(2)^b$	99.31
$\theta(3)^c$	157.79		

[a] $\theta(1)$: dihedral angle between the C(1)–Nb–C(4) plane and the plane of C(1)–C(2)–C(3)–C(4).

[b] $\theta(2)$: dihedral angle between the C(1)–Nb–C(4) plane and the plane of the aromatic ring.

[c] $\theta(3)$: dihedral angle between the C(1)–Nb–C(4) plane and the plane of C(11)–C(15).

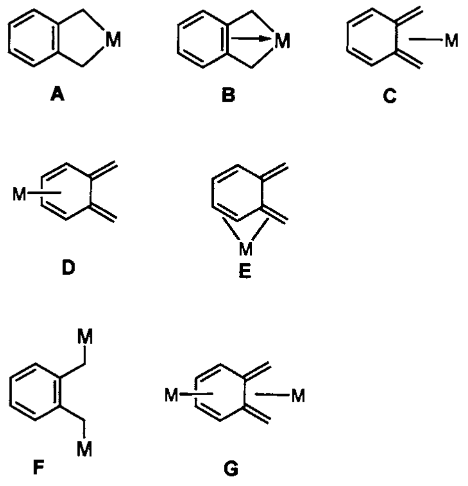

Scheme 2.

consistent with the increased p-character of the 1,4-carbons detected by the ^{13}C NMR, thereby suggesting a larger contribution of the $2\sigma-1\pi$ canonical form compared to the corresponding butadiene complexes.

2.2. Preparation and characterization of tantalum anthracene complexes

Anthracene ligand can coordinate to transition metals in η^4-coordination modes as shown in Scheme 3, where four possible canonical structures (H–K) are given. Here we prepared η^4-anthracene complexes of tantalum with mode I in Scheme 3.

Treatment of Cp^*TaCl_4 with Mg(anthracene)(thf)$_3$ [30–36] gave $Cp^*Ta(\eta^4\text{-}C_{14}H_{10})Cl_2$ (**12**) in 34% yield as green crystals (Eq. (1)). The ^1H NMR spectrum of **12** confirmed that the anthracene coordinated to tantalum via 1–4-carbons. Thus the 1,4-proton signals of the anthracene ligand in **12** were observed at significantly lower field (δ 2.74) due to the aromatic ring system of the anthracene compared to the corresponding butadiene complex, $Cp^*Ta(\eta^4\text{-}C_4H_6)Cl_2$ (**13**) (δ 0.85 and $-$ 0.09) [13], the chemical shift value of 2,3-protons (δ 7.36) being comparable to that of **13** (δ 7.09), along with the observation of a singlet signal due to 9,10-protons at normal aromatic region. The extents of sp^n hybridization of 1,4-carbons (δ 78.6) and 2,3-carbons (δ 125.3) of the anthracene ligand in **12** were calculated by using Newton's empirical law [21] to be $n = 2.33$ and 1.95 (Table 1), respectively.

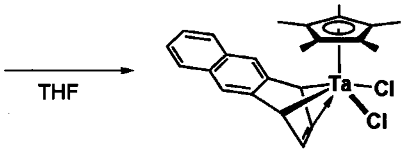

(2)

12

Cp^*TaCl_4 + Mg(anthracene)(thf)$_3$

All attempts failed to obtain a single crystal of **12**. We therefore prepared a benzyl derivative of **12** that would be expected to give better single crystals owing its higher solubility. Reaction of **12** with two equivalents of benzyl Grignard reagent readily gave a dibenzyl complex, $Cp^*Ta(\eta^4\text{-}C_{14}H_{10})(CH_2Ph)_2$ (**14**), in 57% yield (Eq. (3)). The signals of benzyl protons in the ^1H NMR spectrum of **14** appeared at δ 1.46 and 0.13 as an AB quartet and the signals of anthracene protons in **14** are quite similar to those in **12**.

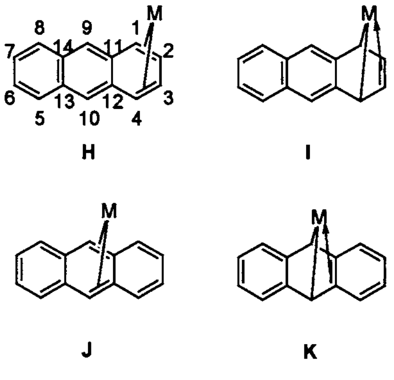

Scheme 3.

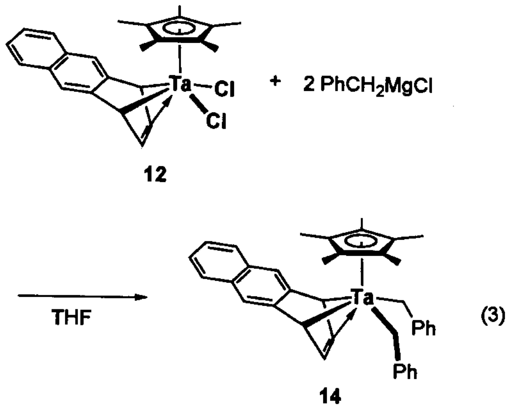

X-ray quality crystals of **14** were obtained from the toluene solution and utilized for structure analysis. An ORTEP drawing of the resulting molecular structure is shown in Fig. 2. The structural data of **14** are summarized in Table 3. Anthracene complexes of iron [37–39] and chromium [40,41] were reported to be η^6-anthracene complexes, while rhodium [42], and zirconium [43] complexes were reported to have η^4-anthracene. In the rhodium complex, anthracene coordinates to the metal at its 1,2,3,4-carbons (type H in Scheme 3), while the zirconocene complex was reported to be bonded at 9,10,11,12-carbons (type J or K in Scheme 3). Complex **14** has type I mode rather than type H in Scheme 3 since the anthracene ligand of **14** is bent at C(1) and C(4), the dihedral angle between the plane defined by C(1)–C(2)–C(3)–C(4) and that defined by C(1)–C(4)–C(11)–C(12) is 133.9°. The C(1)–C(2) (1.444(6) Å), C(2)–C(3) (1.366(7) Å), and C(3)–C(4) (1.453(6) Å) distances of **14** show a long-short-long bond alternation, indicating the stronger contribution of a $2\sigma-1\pi$ canonical form than a 2π canonical structure similar to the conjugated diene complexes of tantalum. In the structurally characterized rhodium complex, $(\eta^5\text{-}C_5H_5)Rh(\eta^4\text{-}C_{14}H_{10})$, the long-short-long bond alternation was also observed but the difference between the C(2)–C(3) distance and the C(1)–C(2) or C(3)–C(4) distances is much smaller compared to that in **14**. The Ta–C(1) and Ta–C(4) distances (av. 2.324 Å) of **14** are longer by 0.06 Å than those of the corresponding butadiene complex, $Cp^*Ta(\eta^4\text{-}C_4H_6)(CH_2Ph)_2$ (**15**). (av. 2.264 Å) [15], while the Ta–C(2) and Ta–C(3) distances (av. 2.365 Å) of **14** are shorter by 0.03 Å than those of **15** (av. 2.391 Å). These findings are attributed to the steric hindrance between the pentamethylcyclopentadienyl and the anthracene ligands. The dihedral angle (85.9°) between the C(1)–Ta–C(2) and C(1)–C(2)–

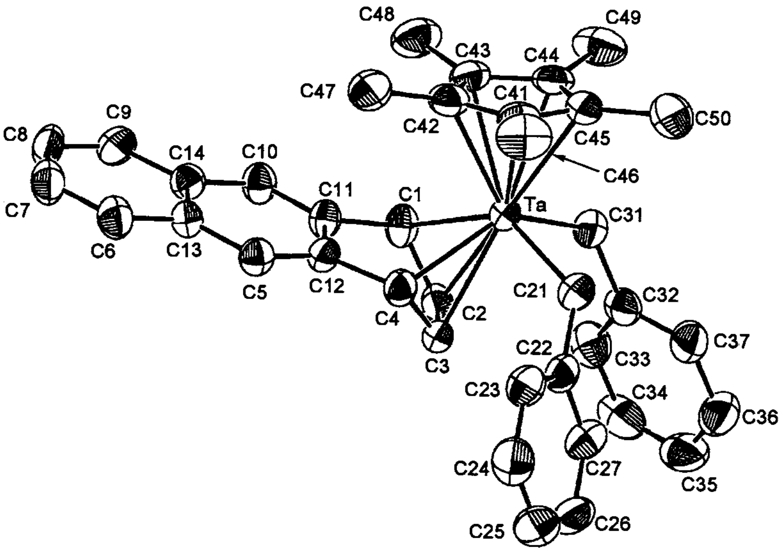

Fig. 2. ORTEP drawing of $Cp^{*}Ta(\eta^4\text{-}C_{14}H_{10})(CH_2Ph)_2$ (**14**) with the numbering scheme.

C(3)–C(4) planes in **14** is smaller than that of **15** (93.3°). The coordination of the pentamethylcyclopentadienyl group is quite normal. The geometry of the two benzyl groups in **14** (Ta–C(21) 2.240(5) Å, Ta–C(31) 2.274(5) Å, Ta–C(21)–C(22) 130.7(3)°, Ta–C(31)–C(32) 125.0(3)°) is also quite similar to that in **15** (Ta–C(21) = 2.249(4) Å, Ta–C(31) = 2.277(4) Å, Ta–C(21)–C(22) = 130.4(3)°, and Ta–C(31)–C(32) = 126.8(3)°) [15].

2.3. *Bonding features of* o*-xylylene and anthracene complexes by NMR and x-ray analysis*

Some examples of *o*-xylylene, anthracene, and butadiene complexes of niobium and tantalum along with some early transition metals are summarized in Table 1, which includes the hybridization degree of the corresponding carbons, dihedral angles between M–C(1)–C(4) and C(1)–C(2)–C(3)–C(4) planes (θ), the difference in M–C distances (Δd) defined by $\Delta d = \{d(\text{M–C(1)}) + d(\text{M–C(4)})\}/2 - \{d(\text{M–C(2)}) + d(\text{M–C(3)})\}/2$, and the difference in C–C distances (Δl) defined by $\Delta l = \{d(\text{C(1)–C(2)}) + d(\text{C(3)–C(4)})\}/2 - d(\text{C(2)–C(3)})$.

The *o*-xylylene complexes generally have higher *p*-content in their sp^n hybridization; in accord with a slightly large θ angle, and a larger negative value of Δd. These indicate a larger contribution of the $2\sigma\text{–}1\pi$ canonical form compared with the butadiene complexes; nevertheless the Δl values of the *o*-xylylene complexes are smaller than that of the butadiene complexes because of the delocalized double bond character of C2–C3 bond owing its aromaticity. In contrast, the bonding of the anthracene ligand is characterized by lower p-content in its sp^n hybridization, a narrower θ angle, and a smaller negative value of Δd; being consistent with the larger contribution of the neutral $2\pi\text{–}\eta^4$-diene canonical form than those of the butadiene complexes as well as the *o*-xylylene complexes. It is notable that the η^4-coordination modes of the *o*-xylylene and anthracene ligands have the opposite electronic properties.

2.4. *Preparation and characterization of niobium cyclooctatetraene complexes*

Recently, Herberich et al. reported half-sandwich cyclooctatetraene complexes of niobium, $(\eta^5\text{-}C_5H_4Me)Nb(\eta^4\text{-}C_4H_6)(C_8H_8)$ (**18**) and $(\eta^5\text{-}C_5H_4Me)Nb(C_8H_8)_2$ (**19**), which were prepared by the ligand exchange reaction of a niobium bis(diene)complex, $(\eta^5\text{-}C_5H_4Me)Nb(C_4H_6)_2$, with cyclooctatetraene [44]. Schrock and coworkers prepared a series of bis(cyclooctatetraene) complexes, $M(C_8H_8)_2R$ (M = Nb, Ta; R = Ph, Me) [45] and tris(cyclooctatetraene) complexes, $[M'][M(C_8H_8)_3]$ (M = Nb, Ta; M′ = K, Li(thf)$_4$, As(C_6H_5)$_4$) by the reduction of metal halides with the cyclooctatetraene dianion [46]. Our synthetic approach was based on the reductive elimination of a dimethyl complex $Cp^{*}Nb(\eta^4\text{-}C_4H_6)Me_2$ (**17**) [14] to form a nascent $Cp^{*}Nb(\eta^4\text{-}C_4H_6)$ that was then trapped by cyclooctatetraene. Treatment of **17** with one equivalent of cyclooctatetraene in THF at 50°C resulted in the formation of $Cp^{*}Nb(\eta^4\text{-}C_4H_6)(C_8H_8)$ (**16**) as purple crystals (Eq. (4)). It is notable that the reaction of **17** with cyclic olefins such as norbornene and acenaphthylene afforded metallacyclobutane derivatives via α-hydrogen elimination of the methyl group bound to the niobium atom [14]. The complex **16** was also obtained by reaction of Cp*Nb(η^4-C$_4$H$_6$)Cl$_2$ with the cyclooctatetraene dianion.

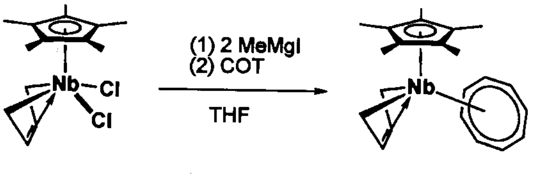

(4)

16

The ^{1}H and ^{13}C resonances due to the COT ligand in **16** are observed as singlet peaks (δ_H 5.16, δ_C 103.6). The ^{13}C chemical shift is at the higher field than that found for uncoordinated COT (δ_C 132.7), but almost comparable with those in (η^5-C$_5$H$_4$Me)Nb(η^4-C$_4$H$_6$)(C$_8$H$_8$) (**18**) (δ_C 101.5) [44], (η^5-C$_5$H$_4$Me)Nb(η^4-C$_4$H$_6$)(C$_8$H$_8$) (**19**) (δ_C 108.3–104.9) [44], and (Pr$^i_2$PC$_2$H$_4$PPr$^i_2$)Ni(η^2-C$_8$H$_8$) (δ_C 103.4) [47], being intermediate between that of uncoordinated COT and that of K$_2$(cot) (δ_C 89.9). Additionally, the coupling constant J_{CH} = 154 Hz of **16** corresponds to that in the free COT (154.5 Hz). All of the η^3-, η^4-, and η^8-cyclooctatetraene ligands in early transition metal complexes generally display one singlet resonance in the ^{1}H NMR spectra, which obviously represents the time average of a dynamic structure since a η^3-C$_8$H$_8$ coordination mode has been determined for **16** in the crystal (see below).

Table 3
Selected bond distances (Å) and angles (°) of **14**

Bond distances (Å)			
Ta–C(1)	2.335(4)	Ta–C(2)	2.371(4)
Ta–C(3)	2.358(4)	Ta–C(4)	2.313(5)
Ta–C(21)	2.240(5)	Ta–C(31)	2.274(5)
Ta–C(41)	2.468(4)	Ta–C(42)	2.463(4)
Ta–C(43)	2.441(4)	Ta–C(44)	2.458(4)
Ta–C(45)	2.447(4)	C(1)–C(2)	1.444(6)
C(2)–C(3)	1.366(7)	C(3)–C(4)	1.453(6)
C(1)–C(11)	1.487(6)	C(4)–C(12)	1.475(6)
C(5)–C(12)	1.373(6)	C(5)–C(13)	1.422(6)
C(6)–C(7)	1.353(7)	C(6)–C(13)	1.414(6)
C(7)–C(8)	1.404(8)	C(8)–C(9)	1.359(7)
C(9)–C(14)	1.421(7)	C(10)–C(11)	1.367(6)
C(10)–C(14)	1.432(6)	C(11)–C(12)	1.406(6)
C(13)–C(14)	1.419(6)		
Bond angles (°)			
C(1)–Ta–C(2)	35.7(2)	C(1)–Ta–C(3)	60.8(2)
C(1)–Ta–C(4)	67.0(2)	C(2)–Ta–C(3)	33.6(2)
C(2)–Ta–C(4)	60.5(2)	C(3)–Ta–C(4)	36.2(2)
Ta–C(1)–C(2)	73.5(3)	Ta–C(2)–C(1)	70.8(2)
Ta–C(1)–C(11)	111.1(3)	Ta–C(4)–C(3)	73.6(3)
Ta–C(3)–C(4)	70.2(2)	Ta–C(4)–C(12)	112.8(3)
C(1)–C(2)–C(3)	115.3(4)	C(2)–C(3)–C(4)	113.6(4)
C(2)–C(1)–C(11)	114.6(4)	C(3)–C(4)–C(12)	114.8(4)
Ta–C(21)–C(22)	130.7(3)	Ta–C(31)–C(32)	125.0(3)
C(21)–Ta–C(31)	94.1(2)		
Fold angles of the best planes (°)			
$\theta(1)^a$	85.86	$\theta(2)^b$	140.27
$\theta(3)^c$	133.86		

[a] $\theta(1)$: dihedral angle between the C(1)–M–C(4) plane and the plane of C(1)–C(2)–C(3)–C(4).

[b] $\theta(2)$: dihedral angle between the C(1)–M–C(4) plane and the plane of C(1)–C(4)–C(11)–C(12).

[c] $\theta(3)$: dihedral angle between the C(1)–C(2)–C(3)–C(4) plane and the plane of C(1)–C(4)–C(11)–C(12).

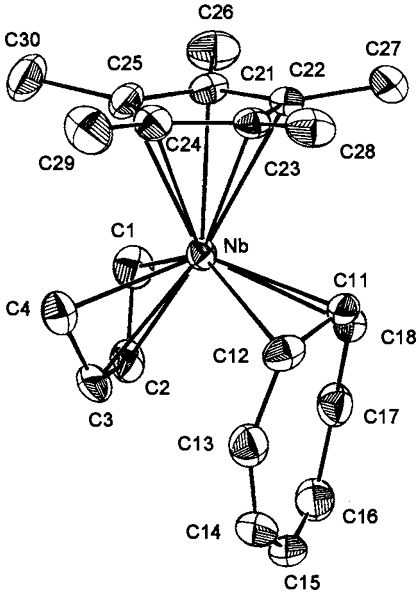

Fig. 3. ORTEP drawing of Cp*Nb(η^4-C$_4$H$_6$)(η^4-C$_8$H$_8$) (**16**) with the numbering scheme.

Whereas a number of transition metal complexes with non planar COT ligands and aromatic planar COT ligands have been reported so far, two complexes bearing a semiaromatic COT ligand, Cp$_2$Ta(η-C$_3$H$_7$)(η^2-C$_8$H$_8$) and (R$_2$PC$_2$H$_4$PR$_2$)Ni(η^2-C$_8$H$_8$) (R = Pr^i, Bu^t) [47], have been described, where a term ‘semiaromatic’ means a planar ring system with bond localization; delocalization corresponding to fully aromatic COT^{2-}. The structure of **16** in crystal has been determined by a single crystal X-ray analysis. Fig. 3 shows a drawing of **16**, which has a η^3-cyclooctatetraene ligand in the solid state. Selected bond distances and angles are summarized in Table 4. It has been reported that the bis(cyclooctatetraene) complex **19** has one η^4-cyclooctatetraene and one η^3-cyclooctatetraene in the solid state. The bonding nature of **16** is quite similar to that found for the η^3-cyclooctatetraene ligand of **19** [44]. The eight C–C bonds of the η^3-cyclooctatetraene ligand in **16** can be classified into two groups; longer C–C bonds including C(11)–(12) (1.411(6) Å), C(11)–(18) (1.415(6) Å), C(12)–C(13) (1.411(6) Å) and C(17)–C(18) (1.406(6) Å), and shorter C–C bonds including C(13)–C(14) (1.385(7) Å), C(14)–C(15) (1.384(7) Å), C(15)–C(16) (1.376(7) Å), C(16)–C(17) (1.392(6) Å). The former group of C–C bonds contain carbons connected to niobium like a η^3-allyl ligand and are lengthened by coordination to the metal. The latter group of short C–C bonds composed of the noncoordinated carbons indicate some contribution of a formal free pentadienyl monoanion. Thus, the niobium metal center should have a formal $+1$ charge to neutralize the formal pentadienyl anion in C_8H_8 forming a formally 16 electron complex.

Since complex **16** has two different kinds of polyolefinic ligands, i.e. butadiene and cyclooctatetraene, the competitive ligand exchange reaction of **16** with diphenylacetylene was investigated. The reaction actually gave $Cp^*Nb(C_8H_8)(PhC{\equiv}CPh)$ (**20**), which has a η^4-cyclooctatetraenyl ligand. The liberation of the butadiene ligand suggests the stronger coordination ability of cyclooctatetraene.

3. Conclusion

We have demonstrated that the *o*-xylylene and anthracene ligands can be used as η^4-ligand alternatives to 1,3-diene ligands for Group 5 transition metals. The newly prepared *o*-xylylene and anthracene complexes were revealed to have structures similar to the butadiene complex by X-ray crystallography. NMR and structural data of the both *o*-xylylene and anthracene complexes indicated that the contribution of the $2\sigma-1\pi$ canonical form is higher than the 2π canonical form but the extent of the contribution of the $2\sigma-1\pi$ canonical form is higher in the *o*-xylylene complexes and lower in the anthracene complexes compared to the corresponding butadiene complexes. NMR spectroscopic measurement of the cyclooctatetraene complexes showed that cyclooctatetraene coordinated to the niobium center in a dynamic coordination mode in solution, while the ligand was found in η^3-fashion in the crystal.

Table 4
Selected bond distances (Å) and angles (°) of **16**

Bond distances (Å)			
Nb–C(1)	2.307(4)	Nb–C(2)	2.424(4)
Nb–C(3)	2.393(4)	Nb–C(4)	2.270(4)
Nb–C(11)	2.255(4)	Nb–C(12)	2.452(4)
Nb–C(18)	2.424(4)	Nb–C(21)	2.441(4)
Nb–C(22)	2.484(4)	Nb–C(23)	2.471(4)
Nb–C(24)	2.436(4)	Nb–C(25)	2.420(4)
C(1)–C(2)	1.415(6)	C(2)–C(3)	1.382(6)
C(3)–C(4)	1.423(6)	C(11)–C(12)	1.411(6)
C(11)–C(18)	1.415(6)	C(12)–C(13)	1.411(6)
C(13)–C(14)	1.385(7)	C(14)–C(15)	1.384(7)
C(15)–C(16)	1.376(7)	C(16)–C(17)	1.392(6)
C(17)–C(18)	1.406(6)		
Bond angles (°)			
Cl(1)–Nb–Cl(2)	92.58(5)	Cl(1)–Nb–C(1)	83.8(2)
Cl(1)–Nb–C(4)	138.9(2)	Cl(2)–Nb–C(1)	137.9(1)
Cl(2)–Nb–C(4)	84.2(2)	C(1)–Nb–C(4)	72.2(2)
Nb–C(1)–C(2)	84.1(3)	Nb–C(4)–C(3)	84.9(3)
C(1)–C(2)–C(3)	115.4(5)	C(2)–C(3)–C(4)	114.2(5)
Fold angles of the best planes (°)			
$\theta(1)$ [a]	101.87		

[a] $\theta(1)$: dihedral angle between the C(1)–M–C(4) plane and the plane of C(1)–C(2)–C(3)–C(4).

4. Experimental Section

4.1. General Procedures

All manipulations involving air- and moisture-sensitive organometallic compounds were carried out by use of the standard Schlenk technique under argon atmosphere. $Cp^*NbCl_2(\eta^4$-buta-1,3-diene) was prepared according to the literature [11]. Hexane, THF, and toluene were dried and deoxygenated by distillation over sodium benzophenone ketyl under argon. Benzene-d_6 was distilled from Na/K alloy and thoroughly degassed by trap-to-trap distillation before use. Cyclooctatetraene purchased from Strem was used as received.

The ^1H (500, 400, and 270 MHz) and ^{13}C (125, 100, and 68 MHz) NMR spectra in C_6D_6 were measured on a JEOL JNM-GX500, a JEOL JNM-GSX400, and a JEOL JNM-EX270 spectrometer. When C_6D_6 was used as the solvent, the spectra were referenced to the residual solvent protons at δ 7.20 in the ^1H NMR spectra and to the solvent carbons at δ 128.0 (triplet for C_6D_6) in the ^{13}C NMR spectra. Assignments for ^1H and ^{13}C NMR peaks for some of the complexes were aided by 2D ^1H-^1H NOESY and 2D ^1H-^{13}C COSY spectra, respectively. Elemental analyses were performed at Elemental Analysis Center, Faculty of Science, Osaka University. All melting points of the complexes were measured in sealed tubes under an argon atmosphere and were not corrected.

4.2. Preparation of $Cp^*Nb[o\text{-}(CH_2)_2C_6H_4]Cl_2$ (1)

To a solution of Cp^*NbCl_4 (0.508 g, 1.37 mmol) in THF (40 ml) cooled at -78°C was added a suspension of *o*-$C_6H_4(CH_2MgCl)_2$ (0.95 equiv, 1.30 mmol) in THF (0.21 M, 6.20 ml) via syringe. The reaction mixture was allowed to warm to room temperature, stirred overnight and evaporated to dryness. The product was extracted with hot hexane (240 ml) at 60°C. Recrystallization from toluene (3.0 ml) at -20°C afforded **1** as green crystals in 16% yield, mp 234.5–237.0°C (dec.). ^1H NMR (270 MHz, C_6D_6, 30°C): δ 0.75 and 1.95 (4H, AB quartet, $^2J_{HH} = 6.1$ Hz, $-CH_2$), 1.80 (15H, s, C_5Me_5), 7.55 (4H, m, C_6H_4). ^{13}C NMR (100 MHz, C_6D_6, 30°C): δ 12.2 (q, $^1J_{CH} = 128$ Hz, C_5Me_5), 71.3 (br t, $^1J_{CH} = 147$ Hz, $-CH_2$), 125.8 (s, C_5Me_5), 131.2 and 137.9 (d, $^1J_{CH} = 161$ and 165 Hz respectively, C_6H_4), 127.3 (s, *ipso*-C_6H_4). Anal. Calcd for $C_{18}H_{23}Cl_2Nb$: C, 53.62; H, 5.75. Found: C, 53.76; H, 5.73.

4.3. Preparation of $Cp^*TaCl_2(\eta^4\text{-}C_{14}H_{10})$ (**12**)

A suspension of anthracenemagnesium (1.08 mmol) in THF (4.5 ml) was added dropwise over a 15 min period to Cp^*TaCl_4 (0.551 g, 1.20 mmol) dissolved in THF (50 ml) at −78°C. The color of the solution changed from orange to dark red. The reaction mixture was stirred for 2 h and then allowed to warm to room temperature. The color of the solution changed from dark red to dark-green. After being evaporated to dryness, the product was extracted with toluene (10 ml) and hexane (500 ml). Recrystallization from toluene (8 ml) at −20°C afforded **2** as dark-green crystals in 34% yield, m.p. 188–190°C (dec). ^{1}H NMR (270 MHz, C_6D_6, 30°C) δ 7.63(m, 2H, 5,8-H of anthracene), 7.36(m, 2H, 2,3-H of anthracene), 7.27(m, 2H, 6,7-H of anthracene), 6.88(s, 2H, 9,10-H of anthracene), 2.74(m, 2H, 1,4-H of anthracene), 1.71(s, 15H, C_5Me_5): ^{13}C NMR(100 MHz, C_6D_6, 30°C) δ 127.1(d, $^1J_{C-H} = 158$ Hz, 5,8-H of anthracene), 125.3 (d, $^1J_{C-H} = 175$ Hz, 2,3-H of anthracene), 125.3 (s, C_5Me$_5$), 124.7 (d, $^1J_{C-H} = 159$ Hz, 6,7-H of anthracene), 121.8(d, $^1J_{C-H} = 158$ Hz, 9,10-H of anthracene), 78.6(d, $^1J_{C-H} = 153$ Hz, 1,4-H of anthracene), 11.2 (q, $^1J_{C-H} = 128$ Hz, C_5Me_5): Anal. Calcd for $C_{24}H_{25}Cl_2Ta$: C, 50.99; H, 4.46. Found: C, 50.91; H, 4.41.

4.4. Preparation of $Cp^*Ta(\eta^4\text{-}C_{14}H_{10})(CH_2Ph)_2$ (**14**)

A solution of $PhCH_2MgCl$ (0.68 mmol) in THF (1.0 ml) was added dropwise over a 20 min period to $Cp^*TaCl_2(\eta^4\text{-}C_{14}H_{10})$ (**12**) (0.167 g, 0.30 mmol) dissolved in THF (40 ml) at −78°C. The reaction mixture was stirred for 30 min and then allowed to warm to room temperature. After being evaporated to dryness, the product was extracted with hexane (180 ml). Recrystallization from toluene (2 ml) and hexane (4 ml) at 0°C afforded **14** as dark-green crystals in 57% yield, m.p. 140–144°C. ^{1}H NMR (270 MHz, C_6D_6, 30°C) δ 7.57 (m, 2H, 5,8-H of anthracene), 7.34 (t, 4H, *m*-H of Ph), 7.23 (m, 2H, 2,3-H of anthracene), 6.97 (t, 2H, *p*-H of Ph), 6.90 (m, 2H, 6,7-H of anthracene), 6.77(d, 4H, *o*-H of Ph), 6.72 (s, 2H, 9,10-H of anthracene), 2.12(m, 2H, 1,4-H of anthracene), 1.59 (s, 15H, C_5Me_5), 1.46 and 0.13 (AB quartet, $^2J_{H-H} = 11.1$ Hz, 4H, CH_2): Anal. Calcd for $C_{38}H_{39}Ta$: C, 67.45; H, 5.81. Found: C, 67.36; H, 5.73.

4.5. Preparation of $Cp^*Nb(\eta^4$-buta-1,3-diene)(cot) (**16**)

To a solution of $NbCl_2Cp^*(\eta^4$-buta-1,3-diene) (0.271 g, 0.768 mmol) in THF (50 ml) cooled at −78°C was added cyclooctatetraene (1.2 equiv, 0.88 mmol) in THF (0.40 M, 2.20 ml) and CH_3MgI (2.3 equiv, 1.74 mmol) in ether (0.62 M, 2.80 ml) via syringe. The reaction mixture was allowed to warm to 20°C, the color of the solution changing from light green to dark green. While the reaction mixture was stirred for 10 h at 50°C, the color of the solution changed from dark green to brown purple. All volatiles were removed under reduced pressure to give a residue, from which the product was extracted with hexane (170 ml). Recrystallization from toluene (4.0 ml) at −20°C afforded **16** as black purple crystals in 42% yield; mp 162–163°C (dec). ^{1}H NMR (400 MHz, C_6D_6, 30°C): δ −0.36 (2H, m, $=CH_2$ anti), 1.48 (15H, s, C_5Me_5), 3.05 (2H, m, $=CH_2$ syn), 4.51 (2H, br, $=CH-$), 5.16 (8H, s, COT). ^{13}C NMR (100 MHz, C_6D_6, 30°C): δ 10.8 (q, $^1J_{CH} = 127$ Hz, C_5Me_5), 53.6 (t, $^1J_{CH} = 149$ Hz, $=CH_2$), 103.6 (d, $^1J_{CH} = 154$ Hz, COT), 110.2 (s, C_5Me$_5$), 126.4 (d, $^1J_{CH} = 163$ Hz, $=CH-$). Anal. Calcd for $C_{22}H_{29}Nb$: C, 68.39; H, 7.57. Found: C, 67.71; H, 7.54.

4.6. Preparation of $Nb(PhC{\equiv}CPh)Cp^*(cot)$ (**20**)

Complex **16** (2.9 mg, 0.008 mmol) was dissolved in 0.3 ml of C_6D_6 in a 5 mm NMR tube. To the dark-purple solution was added PhC≡CPh (1.4 mg, 0.008 mmol) in 0.3 ml of C_6D_6 at 25°C. After the NMR tube was sealed and placed for 5 h in an oil bath heated at 50°C, the ^{1}H NMR was measured. Peaks arising from free butadiene (δ 6.3 and 5.1, m, C_4H_6) were observed together with ones of **20**. ^{1}H NMR (270 MHz, C_6D_6, 30°C): δ 1.43 (15H, s, C_5Me_5), 4.75 (8H, s, COT), 7.11 (2H, overlapped by phenyl signals of free PhC≡CPh peaks), 7.41 (4H, t, $^3J_{HH} = 7.6$ Hz, *m*-Ph), 7.97 (4H, d, $^3J_{HH} = 6.9$ Hz, *o*-Ph).

4.7. Crystallographic Data Collections and Structure Determination of **1**, **14**, and **16**

The crystals of **14** suitable for X-ray diffraction sealed in glass capillaries under argon atmosphere, were mounted on a Rigaku AFC-7R four-circle diffractometer for data collection using Mo–K_α radiation. Three standard reflections were chosen and monitored every 150 reflections. Measured non-equivalent reflections with $I > 3.0\sigma(I)$ were used for the structure determination. Empirical absorption correction was carried out based on an azimuthal scan.

The systematic absences of $h0l$ (l odd) and $0k0$ (k odd) indicate the space group to be $P2_1/c$. The structure was solved by the direct method (SHELXS86) [48] and expanded using standard Fourier maps. In the final refinement cycle (full-matrix), hydrogen atom coordinates were included at idealized positions, and the hydrogen atoms were not refined but were given the same temperature factor as that of the carbon atom to which they were bonded. All calculations were performed using the TEXSAN crystallographic software package. For 428 variable parameters and 5210 observed reflections with $I > 3.0\sigma(I)$, R and R_w values

Table 5
Crystal data and data collection parameters

Complex	**1**	**14**	**16**
Formula	$C_{18}H_{23}Cl_2Nb$	$C_{38}H_{39}Ta$	$C_{22}H_{29}Nb$
Formula weight	403.19	676.67	386.38
Crystal system	Monoclinic	Monoclinic	Monoclinic
Space group	$P2_1/a$ (#14)	$P2_1/c$ (#14)	$P2_1/c$ (#14)
a (Å)	15.119(6)	12.611(4)	12.196(4)
b (Å)	8.253(3)	16.521(3)	11.113(2)
c (Å)	15.502(3)	14.621(3)	14.436(2)
β (°)	115.79(2)	101.65(2)	112.40(1)
V (Å^3)	1741.6(10)	2983(1)	1808.8(6)
Z	4	4	4
D_{calcd}	1.538	1.506	1.419
Radiation	Mo-K$_\alpha$	Mo-K$_\alpha$	Mo-K$_\alpha$
Crystal size (mm)	$0.2\times0.2\times0.1$	$0.4\times0.2\times0.2$	$0.2\times0.2\times0.2$
Abs. coeff (cm^{-1})	0.989	37.03	6.64
Scan mode	ω-2θ	ω-2θ	ω-2θ
Temperature (°C)	23	23	23
Scan speed (° min^{-1})	16	16	8
Scan width (°)	$1.05+0.35\tan\theta$	$0.89+0.35\tan\theta$	$1.42+0.30\tan\theta$
$2\theta_{max}$ (°)	55	55	55
Unique data [$I>3\sigma(I)$]	2519	5210	2835
No. of variables	218	428	264
R	0.034	0.029	0.032
R_w	0.035	0.032	0.036
GOF	1.327	1.28	1.50
Δ (eÅ^{-3})	0.37, −0.40	0.40, −1.38	0.40, −0.50

reached to 0.029 and 0.032, respectively. The pertinent detail of data collection and the final cell dimensions for **14** are given in Table 5.

The molecular structures of **1** and **16** were solved in an essentially similar manner to that of **14**, and only the final parameters were included in Table 5.

Acknowledgements

K.M. acknowledges the support by the Grant-in-Aid for Scientific Research on Priority Area (No. 09238103) from the Ministry of Education, Science, Sports and Culture, Japan and by the Asahi Glass Foundation. A.N. is grateful for the financial support of the Ministry of Education, Science, Sports and Culture of Japan (Specially Promoted Research No. 06101004).

References

[1] D.E. Wigley, S.D. Gray, in: E.W. Abel, F.G.A. Stone, G. Wilkinson (Eds.), Comprehensive Organometallic Chemistry II, vol. 5, Elsevier, Oxford, 1995, p. 57.

[2] K. Mashima, A. Nakamura, J. Organomet. Chem. 500 (1995) 261–267.

[3] A. Nakamura, J. Organomet. Chem. 400 (1990) 35–48.

[4] H. Yasuda, A. Nakamura, Angew. Chem. Int. Ed. Engl. 26 (1987) 723–742.

[5] H. Yasuda, K. Tatsumi, A. Nakamura, Acc. Chem. Res. 18 (1985) 120–126.

[6] G. Erker, C. Krüger, G. Müller, Adv. Organomet. Chem. 24 (1985) 1–39.

[7] H. Yamamoto, H. Yasuda, K. Tatsumi, K. Lee, A. Nakamura, J. Chen, Y. Kai, N. Kasai, Organometallics 8 (1989) 105–119.

[8] H. Yasuda, Y. Kajiwara, K. Mashima, K. Nagasuna, K. Lee, A. Nakamura, Organometallics 1 (1982) 388–396.

[9] Y. Wielstra, S. Gambarotta, A.L. Spek, Organometallics 9 (1990) 572.

[10] J. Blenkers, B. Hessen, F. van Bolhuis, A.J. Wagner, J.H. Teuben, Organometallics 6 (1987) 459–469.

[11] T. Okamoto, H. Yasuda, A. Nakamura, Y. Kai, N. Kanehisa, N. Kasai, J. Am. Chem. Soc. 110 (1988) 5008–5017.

[12] T. Okamoto, H. Yasuda, A. Nakamura, Y. Kai, N. Kanehisa, N. Kasai, Organometallics 7 (1988) 2266–2273.

[13] H. Yasuda, K. Tatsumi, T. Okamoto, K. Mashima, K. Lee, A. Nakamura, Y. Kai, N. Kanehisa, N. Kasai, J. Am. Chem. Soc. 107 (1985) 2410–2422.

[14] K. Mashima, M. Kaidzu, Y. Nakayama, A. Nakamura, Organometallics 16 (1997) 1345–1348.

[15] K. Mashima, Y. Tanaka, M. Kaidzu, A. Nakamura, Organometallics 15 (1996) 2431–2433.

[16] K. Mashima, Y. Tanaka, A. Nakamura, Organometallics 14 (1995) 5642–5651.

[17] K. Mashima, Y. Tanaka, A. Nakamura, J. Organomet. Chem. 502 (1995) 19–23.

[18] K. Mashima, S. Fujikawa, Y. Tanaka, H. Urata, T. Oshiki, E. Tanaka, A. Nakamura, Organometallics 14 (1995) 2633.

[19] K. Mashima, S. Fujikawa, H. Urata, E. Tanaka, A. Nakamura, J. Chem. Soc. Chem. Commun. (1994) 1623–1624.

[20] K. Mashima, S. Fujikawa, A. Nakamura, J. Am. Chem. Soc. 115 (1993) 10990–10991.

[21] M.D. Newton, J.M. Schulman, M.M. Manus, J. Am. Chem. Soc. 96 (1974) 17–23.

[22] G.E. Herberich, U. Englert, K. Linn, P. Roos, J. Runsink, Chem. Ber. 124 (1991) 975–980.

[23] M.A. Bennett, M. Brown, L.Y. Goh, D.C.R. Hockless, T.R.B. Mitchell, Organometallics 14 (1995) 1000–1007.

[24] J.E. McGrady, R. Stranger, M. Bown, M.A. Bennett, Organometallics 15 (1996) 3109–3114.

[25] M.F. Lappert, T.R. Martin, C.L. Raston, B.W. Skelton, A.H. White, J. Chem. Soc. Dalton Trans. (1982) 1959–1964.

[26] M.F. Lappert, T.R. Martin, J.L. Atwood, W.E. Hunter, J. Chem. Soc. Chem. Commun. (1983) 476–477.

[27] M. Mena, P. Royo, R. Serrano, M. Angela, A. Tiripicchio, Organometallics 8 (1989) 476–482.

[28] G.S. Bristow, M.F. Lappert, T.R. Martin, J.L. Atwood, W.F. Hunter, J. Chem. Soc. Dalton Trans. (1984) 399–413.

[29] M.F. Lappert, C.L. Raston, B.W. Skelton, A.H. White, J. Chem. Soc. Chem. Commun. (1981) 485–486.

[30] B. Bogdanovič, N. Janke, H. Kinzelmann, U. Westeppe, Chem. Ber. 121 (1988) 33.

[31] B. Bogdanovič, S. Liao, M. Schwickardi, P. Sikorsky, B. Spliethoff, Angew. Chem. Int. Ed. Engl. 19 (1980) 818.

[32] B. Bogdanovič, S. Liao, R. Mynott, K. Schlichte, U. Westeppe, Chem. Ber. 117 (1984) 1378.

[33] B. Bogdanovič, Angew. Chem. Int. Ed. Engl. 24 (1985) 262.

[34] B. Bogdanovič, N. Janke, C. Kruger, R. Mynott, K. Schlichte, U. Westeppe, Angew. Chem. Int. Ed. Engl. 24 (1985) 960.

[35] T. Alonso, S. Harvey, P.C. Junk, C.L. Raston, B.W. Skelton, A.H. White, Organometallics 6 (1987) 2110.

[36] W.M. Brooks, C.L. Raston, R.E. Sue, F.J. Lincoln, J.J. McGinnity, Organometallics 10 (1991) 2098.

[37] R.G. Sutherland, S.C. Chen, J. Pannekoek, C.C. Lee, J. Organomet. Chem. 101 (1975) 221–229.

[38] W.H. Morrison Jr., E.Y. Ho, D.N. Hendrickson, Inorg. Chem. 14 (1975) 500–506.

[39] W.H. Morrison Jr., E.Y. Ho, D.N. Hendrickson, J. Am. Chem. Soc. 99 (1974) 3603–3608.

[40] B. Deubzer, E.O. Fischer, H.P. Fritz, C.G. Kreiter, N. Kriebitzesch, H.D. Simmons Jr., B.R. Willeford Jr., Chem. Ber. 100 (1967) 3084–3096.

[41] F. Hanic, O.S. Mills, J. Organomet. Chem. 11 (1968) 151–158.

[42] J. Müller, P.E. Gaede, C. Hirsh, K. Qiao, J. Organomet. Chem. 472 (1994) 329–335.

[43] J. Scholz, K.-H. Thiele, J. Organomet. Chem. 314 (1986) 7–11.

[44] G.E. Herberich, U. Englert, P. Roos, Chem. Ber. 124 (1991) 2663–2666.

[45] R.R. Schrock, L.J. Guggenberger, A.D. English, J. Am. Chem. Soc. 98 (1976) 903–912.

[46] L.J. Guggenberger, R.R. Schrock, J. Am. Chem. Soc. 97 (1975) 6693–6700.

[47] I. Bach, K.-R. Pörschke, B. Proft, R. Goddard, C. Kopiske, C. Krüger, A. Rufińska, K. Seevogel, J. Am. Chem. Soc. 119 (1997) 3773–3781.

[48] G.M. Sheldrick, SHELXS86, Program for the Solution of Crystal Structures, Universität Göttingen, 1986.

[49] M. Mena, P. Royo, R. Serrano, M.A. Pellinghelli, A. Tiripicchio, Organometallics 7 (1988) 258–262.